Research Square

Preprints are preliminary reports that have not undergone peer review.
They should not be considered conclusive, used to inform clinical practice,
or referenced by the media as validated information.

Glycyrrhiza uralensis polysaccharides as a DC-based Vaccine Adjuvant: Enhanced Immunotherapy Combined with PD-1 Blockade

Patanmu Aili
Xinjiang University
Shanshan Cai
Xinjiang University
Bei Chen
Xinjiang University
Nuerbiye Aobulikasimu
Xinjiang University
Lili Han
People's Hospital of Xinjiang Uygur Autonomous Region
Adila Aipire
adila16@xju.edu.cn
Xinjiang University

Article

Keywords:

Posted Date: January 23rd, 2026

DOI: https://doi.org/10.21203/rs.3.rs-8390778/v1

License: This work is licensed under a Creative Commons Attribution 4.0 International License.
Read Full License

Additional Declarations: No competing interests reported.

Abstract

The activation of naive $CD8^+$T cells by mature dendritic cells (DCs) through antigen presentation is essential for initiating effective anti-tumor immunity. In our previous study, Glycyrrhiza uralensis polysaccharides (GUPS) were prepared and found that they significantly promoted the maturation and cytokine secretion of human Mo-DC and murine BM-DC through TLR4 signaling pathways. In this study, HPV-DC vaccine prepared with GUPS (GUPS-DC + HPV) significantly suppressed the tumor growth and improved the survival of tumor mice, which was correlated with the induction of HPV-16-specific cellular response and the increased infiltration of $CD8^+$T cells in tumors. Although HPV-DC vaccine can induce CTL response and inhibit tumor growth, the late treatment effect needs to be further improved. Therefore, the combination treatment of HPV-DC vaccine and anti-PD-1 Ab could further improve the therapeutic efficacy, improve the survival rate of tumor mice, generated memory immune response and suppressed lung metastasis of tumors. These findings suggest GUPS as a potent adjuvant that promotes DC maturation, and offering a combination strategy for the treatment of advanced tumors.

1. Introduction

Cancer immunotherapy is currently recognized as a pillar of treatment alongside traditional modalities such as surgery, radiation, and chemotherapy, and it is becoming one of the most exciting and rapidly expanding fields[1-2]. Various forms of immunotherapy, including adoptive cell transfer (ACT), immune checkpoint inhibitors (ICIs), cancer vaccines, oncolytic virus therapy (OVT), have demonstrated significant efficacy and promise[3]. These methods primarily involve inducing CD8+ T cell responses to enhance anti-tumor immunity or restoring the function of exhausted T cells. The presence of anti-tumor cytotoxic T lymphocytes (CTLs) and their infiltration within the tumor microenvironment are prerequisites for treatment efficacy[4-6]. Thus, CD8+ T cells are needed to be primed or back toward effector CTLs for making durable and efficient antitumor immune responses[7-8]. At the forefront of the cancer-immunity cycle, CD8+ T cells priming is essentially a corroborative process involving antigen presenting cells (APCs), including dendritic cells (DCs)[9]. Major histocompatibility complex I (MHC-I) molecules on the surface of DCs are identified by CD8+T cells, which attach to it and scan the surface by crawling over it[10-12]. Furthermore, the upregulation of costimulatory molecules, such as CD40 and CD86, and the release of cytokines during DCs maturation are crucial for establishing stable and enduring interactions with T cells at the immunological synapse (IS). These interactions are vital for T cell expansion and differentiation into memory and effector T cells, thereby underpinning robust cellular immune responses[13-14]. Given the central role of DCs in antitumor immunity, investigators have theorized that DC vaccine would serve as an ideal vaccine platform that can lead to the effective eradication of tumors. The safety and immunogenicity through vaccination potentially constitute a powerful anticancer strategy but clinical benefits have been largely disappointing[15]. New information on the contribution of DCs to tumor immunity should improve DC's maturity in vitro, using adjuvants to optimize their performance in therapeutic applications. Currently approved adjuvants, such as alum and oil, deviate from the purpose for supporting tumor immunotherapy, because they mainly enhance humoral (Th2) immunity and are not

without side effects[16]. The safety of DC vaccines has been fully demonstrated in numerous phase I and II clinical trials, with most DC vaccination regimens exhibiting minimal side effects [17-19]. Studies by Ralph Steinman and Michel Nussenzweig revealed that in vivo targeting of DCs through the conjugation of antigens to antibodies directed against DC surface receptors (such as DEC205 or DCIR) enables efficient antigen delivery and capture by DCs[20]. However, in the absence of adjuvants, targeting DEC205+ DCs in vivo can induce antigen-specific immune tolerance [21]. As observed in the original DEC205 studies, the presence or absence of adjuvants profoundly impacts immune responses. For instance, antigen delivery via CLEC9A-targeting antibodies without adjuvants triggers robust antibody responses associated with Tfh cell differentiation[22], while simultaneously inducing Treg differentiation[23]. To date, only a limited number of cytokines or TLR ligands have been successfully utilized as DC vaccine adjuvants in clinical applications, highlighting the need to identify novel, safe, and potent adjuvants to enhance DC maturation and improve vaccine immunogenicity and clinical efficacy. Consequently, adjuvants play a critical role in enabling DC vaccines to effectively activate T cell immune responses. In recent years, polysaccharides have emerged as promising adjuvant candidates due to their immunomodulatory activities and safety profiles[24-25]. Accumulating evidence demonstrates that polysaccharides can promote dendritic cell maturation, characterized by upregulation of co-stimulatory molecules and cytokines including IL-12[26]. Our previous studies reported the isolation and characterization of Glycyrrhiza polysaccharide (GUPS), which exhibits potent immunostimulatory activity in dendritic cells through TLR4 and downstream p38, JNK, and NF-κB signaling pathways [27-28]. In this study, we adopted GUPS as an adjuvant for human papillomavirus (HPV)-DC vaccine (GUPS-DC+HPV) and evaluated the antitumor response and efficacy of combination therapy with PD-1/PD-L1 inhibitors. The GUPS-DC+HPV effectively inhibited the growth of tumors, resulting in improved the initiation of CTLs, enhanced CD8+ T cell infiltration into tumor sites, and reduced production of regulatory T cells (Tregs) and myeloid-derived suppressor cells (MDSCs). The GUPS-DC+HPV also prolonged the survival rate of mice and suppressed the tumor metastasis. In combination with anti-PD-1, GUPS-DC+HPV further enhanced the antitumor efficacy. Throughout the therapy, GUPS elicited efficient adjuvant activity.

2. Materials and methods

2.1 Materials

G.uralensis polysaccharides (GUPS) were obtained from the Xinjiang Key Laboratory of Biological Resources and Genetic Engineering, Xinjiang University (Urumqi, Xinjiang, China). The purified GUPS had a polysaccharide content of 93% and a molecular weight of 29.1 kDa.Fetal bovine serum (FBS) and Penicillin-streptomycin were purchased from MRC (Changzhou, China). Medium RPMI-1640 medium and phosphate-buffered saline (PBS) were purchased from Gibco (Grand Island, NY, USA). Trypsin was sourced from MRC (China). Granulocyte-macrophage colony-stimulating factor (GM-CSF) was purchased from PeproTech (Rocky Hill, NJ, USA). HPV-16 E6/E7 peptides, including E643–57 (QLLRREVYDFAFRDL), E653–62 (AFRDLCIVYR), E711–20 (YMLDLQPETT), E744–62 (QAEPDRAHYNIVTFCCKCD) and E781–94 (DLLMGTLGIVCPIC), were synthesized by Shanghai Science

Peptide Biological Technology (China). These peptides were dissolved in DMSO at 20 mg/mL, filtered through a 0.22 μm filter membrane, and stored at -80℃. Trizol was purchased from Thermo Fisher Scientific (USA), and reverse transcription reagents were obtained from TAKARA Biotechnology. The Cytofix/Cytoperm kit and Golgi stop (Monensin) were purchased from BD Biosciences (USA). 4% Formaldehyde Fixation Solution was sourced from Biosharp (China). Anti-mouse monoclonal antibodies against PD-1(BE0033-2) and PD-L1 (BE0033-2) were purchased from BioXCell (USA). The antibodies for flow cytometry, including anti-CD25-APC, anti-CD49b-FITC, anti-CD11b-PE, anti-Gr-1-ER780, anti-CD19-APC, anti-CD4-ER780, anti-CD44-PE, anti-Foxp3-PE, anti-CD4-FITC, anti-IFN-γ-APC, were purchased from Elabscience (Wuhan, China). Furthermore, anti-MHC-I-FITC, anti-CD3-APC700, anti-CD8-PE-CY7 and anti-MHC-II-PE, were obtained from BD Biosciences.

2.2 Animals and ethics statement

Female C57BL/6 mice (6-8 weeks old, weighing approximately 22 g) were acquired from the Beijing Laboratory Animal Research Center (Beijing, China) and housed at the temperature-controlled (25˚C) and light-cycled (12-hour light/12-hour dark) in Animal Facility of Xinjiang University (Urumqi, China). All animal experiments in this study were approved by the Ethics Committee on Animal Experiments at the Xinjiang Key Laboratory of Biological Resources and Genetic Engineering (approval number: BRGE-AE001) and were carried out in strict adherence to the guidelines set forth by the Animal Care and Use Committee of the College of Life Science and Technology, Xinjiang University.

2.3 Cell line

The mouse TC-1 cell line was obtained from the Xinjiang Key Laboratory of Biological Resources and Genetic Engineering, Xinjiang University (Urumqi, Xinjiang, China). These cells were cultured in RPMI-1640 medium (Gibco), supplemented with 100 U/ml penicillin, 100 μg/ml streptomycin, and 10% heat-inactivated fetal bovine serum (Gibco). The cells were maintained at 37°C in a humidified incubator with a 5% CO2 atmosphere to ensure optimal growth conditions.

2.4 Vaccine preparation

DCs were collected and cultured for 7 days before being seeded into 60 mm cell culture dishes at a density of 1×10^6 cells/mL, and added GUPS (20 μg/mL) for treatment. After 12 h of incubation, the cells were collected by centrifugation at 1200 rpm for 7 min. Then, the cells were resuspended in fresh medium (1×10^6 cells/mL) and incubation with HPV-16 E6/E7 polypeptide at a final concentration of 10 μg/mL for 2 h, centrifuged (1200 r/min, 7min) to collect, and washed once with PBS. The DCs vaccine prepared by PBS (1×10^6 cells /50 μL) were named GUPS-DC+HPV, and the GUPS-treated DCs were not incubated with HPV-16 E6/E7 polypeptide (GUPS-DC) as a control.

2.5 TC-1 Tumor model and treatment

TC-1 cells, which stably express HPV-16 E6 and E7, were collected during log-phase growth and washed with PBS. TC-1 cells were re-suspended in PBS (1×10^5 cells/mL) and 100 μL of this suspension were subcutaneously injected into the right flank of C57BL/6 mice. The tumor-bearing mice were randomly divided into three groups (6 mice/group) and intradermally injected with 50 μL PBS (control group) or immunized with 1×10^6 cells (GUPS-DC or GUPS-DC+HPV) in 50 μL PBS on day 3 and day 10. Tumor size were measured every other day and tumor volumes were calculated using the formula: tumor volume $(mm3)=(length\times width^2)/2$. At the same time, measuring the weight of the mice every other day. At the end of study, the tumors were isolated, weighted and processed for further analysis. The tumors were fixed, sliced and subjected to hematoxylin and eosin (H&E) staining to evaluate histological changes. Splenocytes were used to detect the immune responses by flow cytometry.

2.6 Survival rate of TC-1 tumor mice

On the 3rd day after the successful establishment of the TC-1 tumor model, the mice were randomly divided into three groups(10 mice/group). On the 3 th and 10 th days, the mice in the treatment groups were given intradermal injection of GUPS-DC or GUPS-DC+HPV, and the untreated group served as the Control group to monitor the survival rate of the tumor mice.

2.7 Flow cytometry

To characterize the phenotype characterization of DCs and T cells, flow cytometry was performed on the isolated splenocytes following staining with specific mAbs. For the analysis of Tregs, the cells were first surface staining with anti-CD4 and anti-CD25 mAbs. Subsequently the cells were fixed and permeabilized using a Foxp3 Staining Buffer Set (eBioscience) and stained with Foxp3 mAbs. To assess antigen-specific $CD8^+$T cell responses, splenocytes (1×10^6 cells/mL) were stimulated with HPV-16 E6/E7 peptides and cultured overnight in the presence of Golgi stop (BD Biosciences). After stimulation, the cells were stained with an anti-CD8 mAbs to identify $CD8^+$T cell. Following surface staining, the cells were fixed and permeabilized using Cytofix/CytopermTM (BD Biosciences) and then stained with IFN-γ mAbs to detect intracellular IFN-γ production. All samples were collected on FACSCalibur (BD Biosciences) and analyzed using the FlowJo platform (Tree Star, Inc, Ashland, OR).

2.8 Hematoxylin and eosin(H&E) staining

Mouse organs were fixed in 4% formaldehyde and then paraffin sections were performed. Sections were stained. Dip the slices into a coconut milk jar filled with mayerhematoxylin and stir for 30 s. Rinse the slide with water for 1 min. Dip the slices into 1% eosin Y solution and stir for 10-30 s. The section was dehydrated in 95% alcohol and 100% alcohol repeatedly, twice for each solution, 30 s each time. Ethanol

is removed with two different xylene compounds. Add one to two drops of medium and cover with mulch. The stained sections were observed with an inverted microscope and photographed.

2.9 RNA-Seq Analysis

Tumor tissues harvested on day 38 were homogenized in TRIzol reagent, and total RNA was extracted according to the manufacturer's instructions. A Bioanalyzer (Agilent) was used to validate the quality and quantity of the purified RNA. Library construction for RNA-seq was performed using the TruSeq Stranded mRNA LT Sample Prep Kit (Illumina), following manufacturer's instructions. The resulting library was then sequenced on a HISeq 2500 platform using the 100 bp single-end protocol (Illumina). Multiple mapped reads were segregated and distributed in a random manner using an in-house script. Reads mapping to protein-coding genes were counted using HTSeq with the GTF file, considering only the protein-coding feature. Differentially expressed genes were examined by DESeq. Genes of interest on pathways annotated in KEGG were selected if their expression levels were significantly different (adjusted $p<0.05$ and ±2-fold change) between the GUPS-DC+HPV and control groups. Read counts were normalized by total number of mapped reads and fit to a standard normal distribution for the depiction of heatmaps.

2.10 Immunohistochemistry

For immunohistochemistry, the tissue sections were deparaffinized, rehydrated, and subsequently incubated in citrate buffer antigen repair buffer (pH 8.0) and 3% H_2O_2, respectively. After blocking with blocking solution for 1 h at room temperature, the sections were incubated for overnight at 4℃ in primary antibody. Following the washes, the sections were then incubated sequentially with the specific secondary antibodies and HRP-conjugated streptavidin. Finally, the sections were stained with 3,3'-diaminobenzidine (DAB) for color development and counterstained with haematoxylinthe. The results were observed and photographed under a fluorescence microscope.

2.11 Combined GUPS-DC+HPV with PD-1/PD-L1 antibody therapy

On the 10th day after the successful establishment of the TC-1 tumor model, the mice were randomly divided into 6 groups(7 mice/group). The untreated group served as the Control group. On the 10th day, intradermal injection of GUPS-DC+HPV was used as the GUPS-DC+HPV group. The mAbPD-L1 (100 μg/mouse) or mAbPD-1 (100 μg/mouse) were intraperitoneally injected into the mAbPD-L1 group and mAbPD-1 group on the 10th, 13th, 16th, 19th and 22nd days, respectively. The combination of GUPS-DC+HPV with mAbPD-1or mAbPD-L1 was divided into the GUPS-DC+HPV+mAbPD-1 or GUPS-DC+HPV+mAbPD-L1 group, and the tumor size was measured every other day, mouse survival rate and immune memory response.

To further test the effect of late treatment, On the 10 th day after the establishment of the TC-1 tumor model, the mice were randomly divided into 4 groups (6 mice/group). The untreated group served as the control group. Starting on the 16th day, intradermal injection of GUPS-DC+HPV was administered to the GUPS-DC+HPV group, with additional injections on the 25th day. The mAbPD-1 group received intraperitoneally injected of mAbPD-1 (100 μg/mouse) on the 16th, 19th, 22nd, 25th and 28th days, respectively. The mice receiving the combination of GUPS-DC+HPV with mAbPD-1 were designated as the GUPS-DC+HPV+mAbPD-1 group, and the tumor size in all groups was measured every other day At the same time, measuring the weight of the mice every other day.

To detect the effect of DC vaccine on tumor recurrences, on day 58, inoculation of TC-1 cells (1×10^5 cells/mouse) from 3 mice in the GUPS-DC+HPV group and GUPS-DC+HPV+mAbPD-1 group. At the same time, naïve mice were inoculated 1×10^5 cells selected as control. The growth of the mouse tumors in the above three groups was examined.

2.12 Lung metastasis models

C57BL/6 mice were injected intravenously with TC-1 cells (1×10^5 cells) on day 0 and were randomly divided into 4 groups(5 mice/group). The untreated group served as control group. On the 3 day, the GUPS-DC+HPV group received an intradermal injection of GUPS-DC+HPV alone. The mAbPD-1 group was intraperitoneally injected with mAbPD-1 (100 μg/mouse) on the 6th, 9th, 12th 15th, 18th, and 21st days, respectively. The mice receiving the combination of GUPS-DC+HPV with mAbPD-1 were designated as the GUPS-DC+HPV+mAbPD-1 group, and the tumor size was measured every other day. On day 21, the mice were euthanized (n=5) and the spleens and lungs were collected for further analysis. The number of pulmonary tumor metastases was then counted.

2.13 Statistical analysis

Data were reported as mean ± standard error of the mean (SEM). One-way analysis of variance (ANOVA), paired or unpaired t-test were used to analyze the statistical significance by Prism5 GraphPad software (GraphPad Software, La Jolla, CA). A value of < 0.05 was considered to be statistically significant.

3. Results

3.1 GUPS improved the antitumor efficacy of HPV-DC vaccine

The adjuvant effect of GUPS on the HPV-DC vaccine was detected in TC-1 tumor mouse model. Tumor mice were treated with GUPS-DC+HPV on day 3 and 10 after injection of TC-1 cells (Fig.1A). As shown in Fig.1B&C, GUPS-DC+HPV markedly inhibited tumor growth compared with control and showed complete

tumor regression in two mice. The H&E staining of tumors showed that the number of tumor cells was dramatically reduced and the necrotic areas were increased in GUPS-DC+HPV group compared with control group (Fig.1D).

The effect of GUPS-DC+HPV on survival rate of tumor mice was further evaluated in another tumor mouse study. Tumor mice were treated with GUPS-DC+HPV on day 3 and 10 after injection of TC-1 cells. Similarly, GUPS-DC+HPV also inhibited tumor growth compared with control (data not shown). On day 54, all mice in the control group had died, and 1 out of 10 mice survived in the GUPS-DC group. Five out of 10 mice were survival in GUPS-DC+HPV group, suggesting that GUPS-DC+HPV greatly improved the survival rate of tumor mice (Fig.1E).

Fig. 1. Tumor growth and tumor mouse survival.

3.2 GUPS-DC+HPV induced the antigen-specific $CD8^+$T cell immune responsese

In light of the excellent anti-tumor activity of the GUPS-DC+HPV, the correlation of antitumor effect and immune responses generated by GUPS-DC+HPV were carried out to explore the infiltration level of myeloid-derived suppressor cells (MDSCs, $CD11b^+Gr\text{-}1^+$), regulatory T cells (iTregs, $CD4^+CD25^-Foxp3^+$ and nTregs, $CD4^+CD25^+Foxp3^+$) and $CD8^+$T ($CD8^+CD44^+$) cells. As expected, Compared to control group, the frequencies of MDSCs and induced Tregs were significantly decreased (Fig.2A&B), and the frequencies of $CD8^+$ T cells and $CD8^+CD44^+$ T cells were notably increased in GUPS-DC+HPV group (Fig. 2C&D). After HPV-16 E6/E7 peptides treatment, HPV-specific cellular responses were detected. As shown in Fig.2E, the frequencies of HPV-specific $CD8^+IFN\text{-}\gamma^+$ T cells markedly increased in GUPS-DC+HPV group compared with control group. Moreover, GUPS-DC+HPV enhanced the infiltration of $CD8^+$T cells in tumors. These results indicated that both the reduction of inhibitory cells and induction of antigen-specific $CD8^+$T cell response contributed to suppressing tumor growth in GUPS-DC+HPV group.

Fig. 2. The immune responses in TC-1 tumor mice after treatment with GUPS-DC+HPV.

In order to elucidate the molecular mechanisms underlying the inhibition of tumor growth by GUPS-DC+HPV, we undertook a comprehensive transcriptomic analysis. Our findings revealed that 2326 differentially expressed genes were identified in the GUPS-DC+HPV group compared to the Control group, with 1810 genes upregulated and 516 genes downregulated ($|\log2 \text{ fold change}| > 0$, $p < 0.001$). Genes with elevated expression were depicted in red, while those with reduced expression were shown in blue (Fig. 3A). From the results of GO enrichment analysis, the most significant 10 Term plots are displayed, and the size and color of points correspond to the number of genes annotated to GO Term and the significance (Fig. 3B). Concomitantly, numerous pathways related to anti-tumor immunity were

upregulated in the GUPS-DC+HPV (Fig. 3C). In particular, cytokine-cytokine receptor interaction, chemokine signaling, cell adhesion molecules and nature killer cell mediated cytotoxicity (Fig.3C).

Fig.3. RNA-seq analysis of the expression profiles of differentially expressed genes in immune-related pathways.

In nature killer cell mediated cytotoxicity pathway，cytotoxicity associated genes，including *Fas*, *GzmB*, *Prf1*, *CD244*, were significantly increased in response to GUPS-DC+HPV(Fig. 4A). Immunohistochemical data also showed GzmB and Fas upregulated in tumor tissue in the GUPS-DC+HPV treatment group. On the other hand, BCL-2 was decreased with the GUPS-DC+HPV therapy (Fig. 4C). In addition, numerous genes related to cytokine-cytokine receptor interaction were upregulated, such as *Ifng, Ccl10, Ccl14, Il15, and Il17,* were significantly increased in response to GUPS (Fig. 4B). The expression of TNF-α was increased compared with the control group. Taken together, these results strongly suggest that GUPS-DC+HPV therapy elicits Th1-type anti-tumor immunity with essential cytokine induction.

Fig.4. Perform RNA sequencing analysis on the expression profiles of differentially expressed genes in immune-related pathways.

However, it was worth noting that the high expression levels of CD274 was observed, which might express on the surface of tumor cells and activated APCs (Fig. 4A). Next, we devised a combination therapy with GUPS-DC+HPV and anti-PD-L1 Ab or anti-PD-1 Ab against TC-1 tumors.

3.3 GUPS-DC+HPV combined with anti-PD-1/PD-L1 Ab therapy further inhibited tumor growth and improved memory immune response and survival in tumor mice

Although the mechanism of action of DC vaccine is clear, the tumor immune microenvironment and tumor immunosuppressive mechanisms greatly limit the effect of DC tumor vaccine. Therefore, we established a TC-1 tumor mouse model and evaluated the anti-tumor effect of GUPS-DC+HPV vaccine combined with PD-1 and PD-L1 blocking antibodies in the treatment of advanced tumor mice. The mice were given GUPS-DC+HPV vaccine on the 10 th day after inoculation of TC-1 cells, and the mice were given 100 μg of mAbPD-1 or mAbPD-L1 on the 10, 13, 16, 19 and 22 th days (Fig. 5A). Tumor size was measured every other day. At the same time, measuring the weight of the mice every other day. It is found that GUPS-DC+HPV, mAbPD-1 and mAbPD-L1 significantly inhibited tumor growth and had no significant effect on the weight of mice, with no significant side effects on the mice (Fig. 5B). When all the mice in the control group died, the survival rate of the GUPS-DC+HPV group was 75% (Fig. 5C). The survival rate of the GUPS-DC+HPV+mAbPD-1 group was 87.5% (Fig. 5C). The survival rate of the GUPS-DC+HPV+mAbPD-L1 group was only 50%. In the mAbPD-1 group, only one mouse survived, and in the mAbPD-L1 group, only two mice survived. Compared with the control group, GUPS-DC+HPV+mAbPD-1 significantly improved the survival rate (Fig. 5C). These results indicated that GUPS-DC+HPV combined

with mAbPD-1 could significantly improve the probability of survivability in mice. On day 58, mice whose tumors had completely disappeared in the GUPS-DC+HPV group and the GUPS-DC+mAbPD-1 combination group were selected for the second inoculation with TC-1 cells. Naive mice of the same age were also inoculated with TC-1 cells as controls. The results showed that there were no tumors in GUPS-DC+HPV group and GUPS-DC+HPV+mAbPD-1 vaccine combination group, indicating that the vaccine and combination treatment induced memory immune response in mice (Fig.5D). The above results indicated that the combination of HPV-DC vaccine and PD-1 blocking antibody significantly inhibited the growth of TC-1 tumors, produced a strong memory immune response, improved the survival rate of mice.

At present, HPV-DC vaccine research and development is becoming more mature. With the increases of HPV vaccine coverage, the incidence of a disease related to HPV is gradually reduced. However, in the late stage of cancer, advanced cancer cells have spread throughout the body, and conventional treatments were ineffective, so we established a late treatment model to evaluate its anti-tumor effect, 10 days after the establishment of TC-1 tumor model, patients were randomly divided into 4 groups, 5 cases in each group. The untreated group was used as control group. On day 16, GUPS-DC+HPV was injected intraderally as GUPS-DC+HPV group. The mAbPD-1 group received intraperitoneal injection of mAbPD-1 (100 μg/animal) at 16, 19, 22, 25, and 28 th days respectively. The GUPS-DC+HPV+mAbPD-1 combination treatment was divided into the GUPS-DC+ HPV+mAbPD-1 group, and tumor size was measured every other day (Fig. 5E). The results showed that HPV-DC+mAbPD-1 treatment induced durable, objective tumor regression and immune response in patients (Fig. 5F). The above results suggest that the combination therapy of HPV-DC and PD-1/PD-L1 is a safe, effective and feasible treatment strategy, which will bring new hope for patients with HPV infection.

Fig.5. Treatment of tumor mice by GUPS-DC+HPV combined with mAbPD-1 or mAbPD-L1.

3.4 The role of GUPS-DC+HPV combined with PD-1 antibody in the treatment of lung metastases

The lungs are the main site of metastatic spread. Due to their extensive vascularization and large surface area, which is essential for normal lung function, tumors have many opportunities to stop, extravasate, and colonize this organ. The poor prognosis of patients with recurrent and metastatic cervical cancer has always been a daunting challenge for clinicians. Thus, we developed a tumor lung metastasis model. The untreated group was used as control group. On the 3 th day, GUPS-DC+HPV was given intradermal injection alone was the GUPS-DC+HPV group. mAbPD-1 (100 μg/animal) were intraperitoneally injected into the mAbPD-1 group, on the 6, 9, 12、15, 18, and 21th days respectively (Fig. 6A). It was found that after the tumor cells were injected through the tail vein, they reached the lungs of the mice through the blood vessels and formed lung metastases. Compared with the control group, HPV-DC, mAbPD-1 alone and HPV-DC combined with mAbPD-1 significantly reduced the number of lung metastases, and the HPV-DC combined with mAbPD-1 had the best effect (Fig. 6B). MDSCs and Tregs

contribute to tumor growth and the inhibition of antitumor immune responses[29-32]. On day 21, the spleens were collected to detect the immune cells and found that the GUPS-DC+HPV, mAbPD-1 and GUPS-DC+HPV+mAbPD-1 groups significantly reduced the proportion of Tregs cells and significantly increased the proportion of activated CD4+ and $CD8^+$T cells compared with the control group(Fig. 6C). The combination of HPV-DC to PD-1 blocking antibodies provides an inhibitory environment for the tumor microenvironment, which regulate immunosuppression and activates immune cells. Therefore, the reduction of inhibitory cells and induction of $CD8^+$T cell response together inhibited tumor growth in GUPS-DC+HPV+mAbPD-1 group, and proposing a new therapeutic strategy for the treatment of cervical cancer.

Fig.6. GUPS-DC+HPV combined with mAbPD-1 or mAbPD-L1 to treat lung metastatic tumor mice.

4. Conclusion

Although a large number of clinical trials have proved that DC vaccine has the advantages of high safety and induced antigen-specific immune response, its clinical efficacy needs to be improved, especially the insufficient maturity of DC in vitro, resulting in the limited degree of immune response[33-35]. Therefore, this study used GUPS as an adjuvant of HPV-DC vaccine to improve the immunogenicity of the vaccine. Following vaccination of normal C57BL/6 mice and stimulating HPV-DC prepared from mature DC with GUPS, the vaccine significantly enhanced $CD8^+$T cell activation and antigen-specific CTL response compared with the HPV vaccine prepared from immature DC, which not only inhibited tumor growth but also increased survival of tumor mice. Transcriptome data revealed that compared to the control group, the GM-DC+HPV group exhibited upregulation of numerous anti-tumor immune-related pathways, particularly cytokine-cytokine receptor interactions, chemokine signaling, cell adhesion molecules, and natural killer (NK) cell-mediated cytotoxicity. Notably, genes associated with cytokine-cytokine receptor interactions—including *Ifng, Ccl10, Ccl14, Il15,* and *Il17*—were significantly upregulated. Within the NK cell-mediated cytotoxicity pathway, cytotoxic-related genes such as *Fas, GZMB, Prf1, and CD244* also showed increased expression. These findings strongly suggest that GM-DC+HPV therapy induces a Th1-polarized anti-tumor immune response by activating key cytokines. However, further functional gene analysis revealed elevated expression of CD274 (PD-L1) in the GM-DC+HPV group, indicating persistent immunosuppressive signals within the tumor microenvironment (TME).

Traditionally, cancer was attributed to the accumulation of oncogenic and tumor suppressor gene mutations. However, recent paradigm shifts have established the TME as a critical driver of tumor progression. The TME comprises diverse cellular components—lymphocytes, immune cells, cancer-associated fibroblasts, endothelial cells, pericytes, and tissue-resident cells—These host cells were once considered bystanders in tumorigenesis, but they are now known to play a critical role in cancer progression[36]. Tumor cells evade immune surveillance through multiple mechanisms: loss of tumor antigen expression or downregulation of MHC-I molecules, secretion of immunosuppressive cytokines (*IL-10, TGF-β*), expansion of regulatory T cells (Tregs) and myeloid-derived suppressor cells (MDSCs),

activation of immune-inhibitory pathways, and overexpression of immune checkpoint molecules such as *PD-1*, *BTLA*, and *CTLA-4*[37]. Overcoming TME-induced immune tolerance/suppression thus demands novel therapeutic strategies.

Tumor cells frequently overexpress PD-L1 to suppress T-cell cytotoxicity and evade CTL-mediated killing[38-40], making immune checkpoint inhibitors a focal point in cancer immunotherapy. FDA-approved CTLA-4 and PD-1/PD-L1 inhibitors have demonstrated clinical efficacy, while next-generation checkpoint inhibitors (IDO inhibitors)[41] are under clinical investigation. Rigo et al[42]. reported that combined anti-PD-L1/PD-1 and anti-CD4 immunotherapy achieved cure in syngeneic disseminated neuroblastoma. In non-small cell lung cancer, radiotherapy synergized with anti-PD-L1 antibodies to enhance antitumor responses[43]. Ren et al[44]. further demonstrated that imiquimod potentiates the therapeutic effect of exogenous BM-DC vaccines in murine melanoma.Massarelli et al[45]. reported that ISA101, an HPV-16 synthetic long peptide vaccine combined with nivolumab, a PD-1 immune checkpoint inhibitor, exhibited promising efficacy outcomes in patients with recurrent HPV-16–positive cancer. the statistical power was reduced to77.6%. with anORR of 33% and responses were durable with63%. Liuet al[46]. reported that Combinatorial therapy with ADEC205-SC-E7 vaccine and anti-PD-L1 blockade showed significantly enhanced therapeutic effects. Penget al[47]. reported that intratumoral injection of TA-CIN vaccine can induce a strong E7-specific CD8+T cell response both locally and systemically. When combining the intratumoral TA-CIN vaccine with PD-1 blockade, combination therapy has much stronger antitumor effects compared to either TA-CIN vaccination or anti-PD-1 antibody administration alone.

We designed a combination therapy integrating GM-DC+HPV with anti-PD-L1 or anti-PD-1 antibodies for TC-1 tumor treatment. As we expected, GUPS-DC+HPV, mAbPD-1 and mAbPD-L1 significantly inhibited tumor growth and had no significant effect on the weight of mice, with no significant side effects on the mice. The survival rate of the GUPS-DC+HPV+mAbPD-1 group was 87.5% and produced a strong memory immune response. Consistently, we also observed that Compared with the control group, HPV-DC, mAbPD-1 alone and HPV-DC combined with mAbPD-1 significantly reduced the number of lung metastases.

GUPS demonstrate significant potential in immunomodulation, antitumor activity, and chronic disease management. However, current clinical applications of GUPS are predominantly limited to adjuvant therapy, such as alleviating cancer-related fatigue and chemotherapy-induced side effects. Their potential as standalone therapeutic agents still requires validation through large-scale clinical trials. Future efforts must focus on advancing clinical translational research, overcoming technical bottlenecks, and facilitating its transition from laboratory research to clinical practice. As an adjuvant for human papillomavirus (HPV)-dendritic cell (DC) vaccines, GUPS enhances antigen-specific immune responses, promotes $CD8^+$T cell infiltration into tumor tissues, suppresses tumor growth, and improves survival rates in tumor-bearing mice. The combination of mAbPD-1 and GUPS-DC+HPV further enhanced anti-tumor efficacy and increased the survival rate of mice . These findings provide a critical research foundation for developing therapeutic vaccines and combination strategies, potentially benefiting

patients with advanced, recurrent, or metastatic cervical cancer and offering robust data support for clinical investigations.

Abbreviations

BM, bone marrow; CTL, cytotoxic T lymphocytes; DC, dendritic cell; GUPS *Glycyrrhiza uralensis polysaccharides;* HPV, human papillomavirus; LN, lymph node; Th cell, T helper cell.

Declarations

Conflict of Interest

The authors declare that the research was conducted in the absence of any commercial or financial relationships that could be construed as a potential conflict of interest.

Ethics Statement

Approval of the research protocol by an Institutional Review Board: Ethics Committee-approved protocols (XJUAE-2023-030).

Author Contributions

PA: Writing–original draft, Conceptualization, Data curation, Formal Analysis, Methodology, Validation. SC: Writing–original draft, Data curation Methodology, Validation. BC: Writing–review & editing, Conceptualization. NA: Writing–original draft, Conceptualization, Visualization. LH: Validation, Supervision, Funding acquisition, Conceptualization. AA: Writing–review & editing, Validation, Supervision, Funding acquisition, Conceptualization.

Funding

This work was supported by the Key research and development program in Xinjiang Uygur Autonomous Region (2022B03018-5) and the Natural Science Foundation of Xinjiang Uygur Autonomous Region (2022D01C97), Fudan University Ministry of Education / National Health Commission / Academy of Medical Sciences Key Laboratory of Molecular Virology Open Projects (FDMV-2024003) and the Jiayin Hospital Horizontal Project (No. 202306140004) .

Data Availability Statement

The original contributions presented in the study are included in the article, further inquiries can be directed to the corresponding authors.

References

1. Igarashi Y, Sasada T. Cancer Vaccines: Toward the Next Breakthrough in Cancer Immunotherapy[J]. J Immunol Res. 2020 Nov 17;2020:5825401.
2. Riley RS, June CH, Langer R. Delivery technologies for cancer immunotherapy[J]. Nat Rev Drug Discov. 2019 Mar;18(3):175-196.
3. Zhang Y, Zhang Z. The history and advances in cancer immunotherapy: understanding the characteristics of tumor-infiltrating immune cells and their therapeutic implications[J]. Cell Mol Immunol 17, 807–821 (2020).
4. Giles JR, Globig AM, Kaech SM. $CD8^+$ T cells in the cancer-immunity cycle[J]. Immunity. 2023 Oct 10;56(10):2231-2253.
5. Rui R, Zhou L, He S. Cancer immunotherapies: advances and bottlenecks[J]. Front Immunol. 2023 Aug 24;14:1212476.
6. Farhood B, Najafi M, Mortezaee K. $CD8^+$ cytotoxic T lymphocytes in cancer immunotherapy: A review[J]. Cell Physiol. 2019 Jun;234(6):8509-8521.
7. Philip M, Schietinger A. $CD8^+$ T cell differentiation and dysfunction in cancer[J]. Nat Rev Immunol. 2022 Apr;22(4):209-223.
8. Wang Q, Qin Y, Li B. $CD8^+$ T cell exhaustion and cancer immunotherapy[J]. Cancer Lett. 2023 Apr 10;559:216043.
9. Park HY, Ashayeripanah M, Chopin M. Harnessing dendritic cell diversity in cancer immunotherapy[J]. Curr Opin Immunol. 2023 Jun;82:102341.
10. Sadeghzadeh M, Bornehdeli S, Mohahammadrezakhani . Dendritic cell therapy in cancer treatment; the state-of-the-art[J]. Life Sci. 2020 Aug 1;254:117580.
11. Hiam-Galvez KJ, Allen BM, Spitzer MH. Systemic immunity in cancer[J]. Nat Rev Cancer. 2021 Jun;21(6):345-359.
12. Kang B.H, Lee H.K. Dendritic Cell-Based Immunotherapy in Hot and Cold Tumors[J]. Int. J. Mol. Sci. 2022, 23, 7325.
13. Kalinski P. Dendritic cells in immunotherapy of established cancer: Roles of signals 1, 2, 3 and 4. Curr Opin Investig Drugs[J]. 2009 Jun;10(6):526-35.
14. Sabado RL, Balan S, Bhardwaj N. Dendritic cell-based immunotherapy[J]. Cell Res. 2017 Jan;27(1):74-95.
15. Harari A, Graciotti M, Bassani-Sternberg M. Antitumour dendritic cell vaccination in a priming and boosting approach. Nat Rev Drug Discov[J]. 2020 Sep;19(9):635-652.
16. McKee AS, Marrack P. Old and new adjuvants. Curr Opin Immunol[J]. 2017 Aug;47:44-51.

17. Schreibelt G, Bol KF, Westdorp H, et al. Effective clinical responses in metastatic melanoma patients after vaccination with primary myeloid dendritic cells [J]. Clinical cancer research an official journal of the american association for cancer research, 2015, 22(9):2155-2166.
18. Schadendorf D, Ugurel S, Schuler-Thurner B, et al. Dacarbazine (DTIC) versus vaccination with autologous peptidepulsed dendritic cells (DC) in first-line treatment of patients with metastatic melanoma: a randomized phase III trial of the DC study group of theDeCOG [J]. Ann Oncol, 2006, 17:563-570.
19. Beer TM, Bernstein GT, Corman JM, et al. Randomized trial of autologous cellular immunotherapy with sipuleucel-T in androgen-dependent prostate cancer [J]. Clin Cancer Res, 2011, 17:4558-4567.
20. Soares H, Waechter H, Glaichenhaus N, et al. A subset of dendritic cells induces CD4+T cells to produce IFN-γ by an IL-12-independent but CD70-dependent mechanism in vivo [J]. Exp Med, 2007, 204(5):1095-1106.
21. Hawiger D, Inaba K, Dorsett Y, et al.Dendritic cells induce peripheral T cell unresponsiveness under steady state conditions in vivo [J]. J Exp Med, 2001, 194:769-780.
22. Poulin LF, Salio M, Griessinger E, et al. Characterization of human DNGR-1 + BDCA3 + leukocytes as putative equivalents of mouse CD8alpha+ dendritic cells [J]. J Exp Med, 2010, 207:1261–1271.
23. Kikete S. et al. Plant-derived polysaccharides activate dendritic cell-based anti-cancer immunity[J]. Cytotechnology 70, 1097-1110 (2018).
24. Li, J. & Zhang F et al. . The immunoregulatory effects of Chinese herbal medicine on the maturation and function of dendritic cells[J]. Journal of ethnopharmacology 171, 184-195, 2015.05.050 (2015).
25. Li, J. et al. Purification, characterization and bioactivities of polysaccharides from Pleurotus ferulae[J]. Food Funct 8, 1905-1914 (2017).
26. Aipire A, Mahabati M, Cai S. The immunostimulatory activity of polysaccharides from Glycyrrhiza uralensis[J]. PeerJ. 2020 Jan 29;8:e8294.
27. Aipire A, Li J, Yuan P. Glycyrrhiza uralensis water extract enhances dendritic cell maturation and antitumor efficacy of HPV dendritic cell-based vaccine[J]. Sci Rep. 2017 Mar 8;7:43796.
28. Aipire A, Yuan P, Aimaier A. Preparation, Characterization, and Immuno-Enhancing Activity of Polysaccharides from Glycyrrhiza uralensis. Biomolecules[J]. 2020 Jan 19;10(1):159.
29. Jaafar F. et al. Correlation of CXCL12 expression and FoxP3^{+} cell infiltration with human papillomavirus infection and clinicopathological progression of cervical cancer[J]. The American journal of pathology 175, 1525-1535.
30. Kryczek I. et al. FOXP3 defines regulatory T cells in human tumor and autoimmune disease[J]. Cancer Res 69, 3995-4000.
31. Gabrilovich D. I. & Nagaraj, S, et al.. Myeloid-derived suppressor cells as regulators of the immune system[J]. Nat Rev Immunol 9, 162-174 (2009).
32. Sica A. & Bronte V, et al . Altered macrophage differentiation and immune dysfunction in tumor development[J]. J Clin Invest 117, 1155-1166 (2007).

33. De Visser KE, Joyce JA et al. ,. The evolving tumor microenvironment: From cancer initiation to metastatic outgrowth. Cancer Cell[J]. 2023 Mar 13;41(3):374-403. 2023.02.016.
34. Lanitis E, Irving M, CoukosG, et al. Targeting the tumor vasculature to enhance T cell activity[J].Curr Opin Immunol, 2015, 33:55-63.
35. Anguille, Sébastien, Smits EL, et al. Clinical use of dendritic cells for cancer therapy[J]. The Lancet Oncology, 2014, 15(7):e257-e267.
36. Mastelic-Gavillet B, Balint K, Boudousquie C, et al. Personalized Dendritic Cell Vaccines- Recent Breakthroughs and Encouraging Clinical Results[J]. Front Immunol. 2019,10:766.
37. João Constantino, Célia Gomes, Amílcar Falcão , et al. Antitumor dendritic cell-based vaccines: Lessons from 20 years of clinical trials and future perspectives[J]. Translational Research, 2016, (168):74-95.
38. Yang MW, Fu XL, Jiang YS, et al. Clinical significance of programmed death 1/programmed death ligand 1 pathway in gastric neuroendocrine carcinomas[J]. World Journal of Gastroenterology, 2019, 25(14):1684-1696.
39. Duverger L, Amélie Osio, Cribier B, et al. Heterogeneity of PD-L1 expression and CD8 tumor-infiltrating lymphocytes among subtypes of cutaneous adnexal carcinomas[J]. Cancer Immunology, Immunotherapy, 2019:1-10.
40. Yu D, Cheng J, Xue K, et al. Expression of Programmed Death-Ligand 1 in Laryngeal Carcinoma and its Effects on Immune Cell Subgroup Infiltration[J]. Pathology & Oncology Research, 2018.
41. Sanchez-Paulete AR, Cueto FJ, Martinez-Lopez M, et al. Cancer immunotherapy with immunomodulatory anti-CD137 and anti-PD-1 monoclonal antibodies requires BATF3 -dependent dendritic cells [J]. Cancer Discov, 2016, 6:71-79
42. Rigo V, Emionite L, Daga A, et al. Combined immunotherapy with anti-PDL-1/PD-1 and anti-CD4 antibodies cures syngeneic disseminated neuroblastoma[J]. Scientific Reports, 2017, 7(1):14049.
43. Gong X, Li X, Jiang T, et al. Combined Radiotherapy and Anti-PD-L1 Antibody Synergistically Enhances Antitumor Effect in Non-Small Cell Lung Cancer[J]. Journal of Thoracic Oncology Official Publication of the International Association for the Study of Lung Cancer, 2017, 12(7):1085-1097.
44. Shurong R, Qiubo W, Yanli Z, et al. Imiquimod enhances the potency of an exogenous BM-DC based vaccine against mouse melanoma[J]. International Immunopharmacology, 2018, 64:69-77.
45. Massarelli E, William W, Johnson F, et al. Combining Immune Checkpoint Blockade and Tumor-Specific Vaccine for Patients With Incurable Human Papillomavirus 16-Related Cancer: A Phase 2 Clinical Trial[J]. JAMA Oncol. 2019 Jan 1;5(1):67-73.
46. Liu Z, Zhou H, Wang W,et al. A novel dendritic cell targeting HPV16 E7 synthetic vaccine in combination with PD-L1 blockade elicits therapeutic antitumor immunity in mice[J]. Oncoimmunology. 2016 Mar 10;5(6):e1147641.
47. Peng S, Tan M, Li YD,et al. PD-1 blockade synergizes with intratumoral vaccination of a therapeutic HPV protein vaccine and elicits regression of tumor in a preclinical model[J]. Cancer Immunol Immunother. 2021 Apr;70(4):1049-1062.

Figures

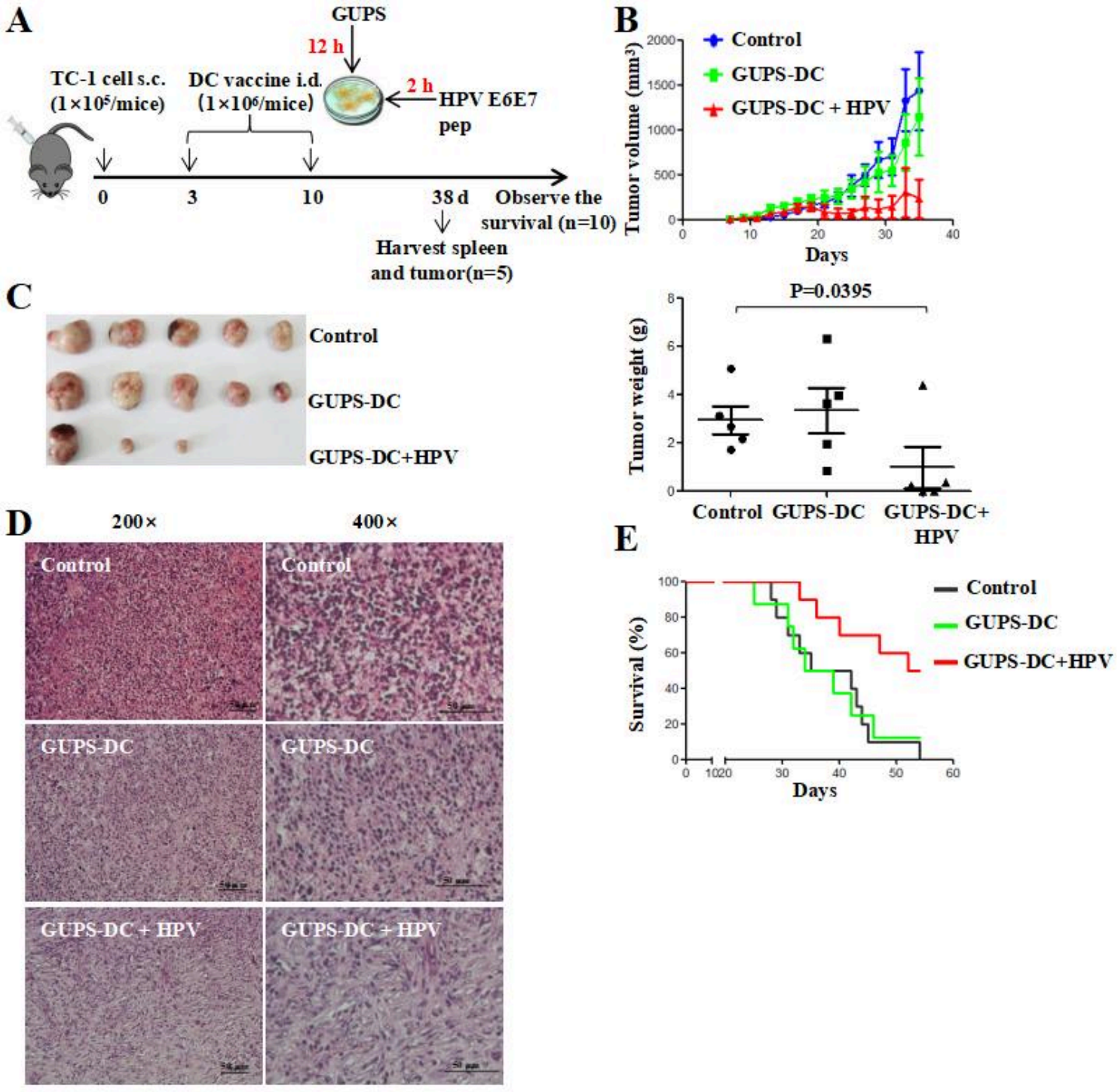


Figure 1

Tumor growth and tumor mouse survival.BM-DC were treated with GUPS for 12 h, then pulsed with HPV-16 E6/E7 peptides (GUPS-DC+HPV). Tumor mice were treated with GUPS-DC+HPV on day 3 and 10 after injection of TC-1 cells (A). Tumor growth curves reflected by the average tumor volume during the period of immunization (B). Tumors were isolated and weighted on day 38. The tumor photo and weight are shown in upper and lower panels, respectively. The p value was indicated (unpaired t-test) (C). H&E

staining images of tumor tissues (D). The survival of tumor mice after GUPS-DC+HPV treatment. Tumor mice were treated with GUPS-DC+HPV on day 3 and 10, then the survival of tumor mice was monitored (E).

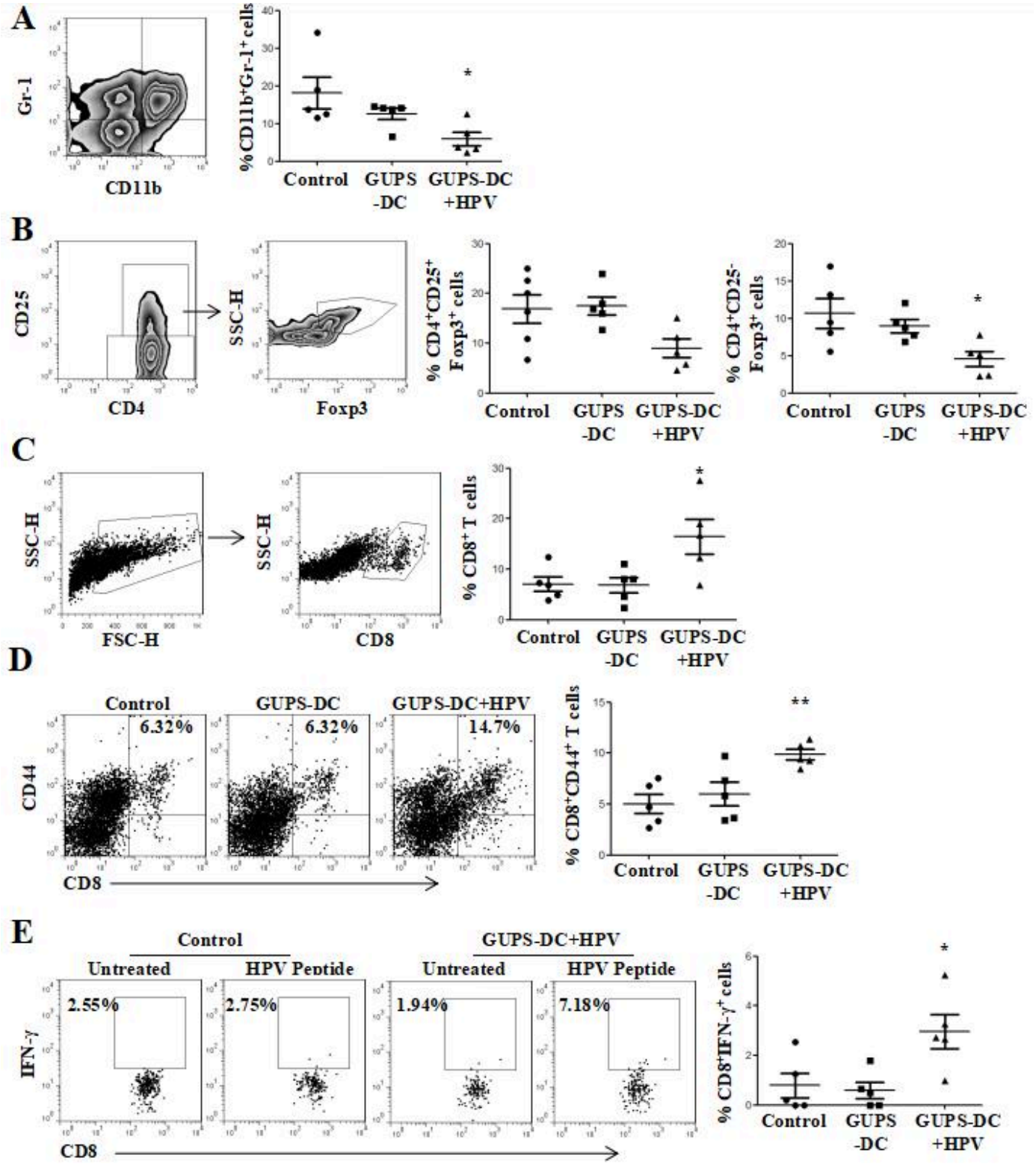


Figure 2

The immune responses in TC-1 tumor mice after treatment with GUPS-DC+HPV. On day 38, splenocytes were isolated to analyze the frequencies of MDSCs (A), iTregs and nTregs (B), $CD8^+$T cells (C) and $CD8^+CD44^+$ T cells (D). Splenocytes were stimulated with HPV-16 E6/E7 peptides overnight in the presence of Golgi stop. The frequency of antigen specific $CD8^+IFN\text{-}\gamma^+$T cells was analyzed by flow cytometry (E).(*P < 0.05, **P < 0.01, ***P < 0.001 versus the control group).

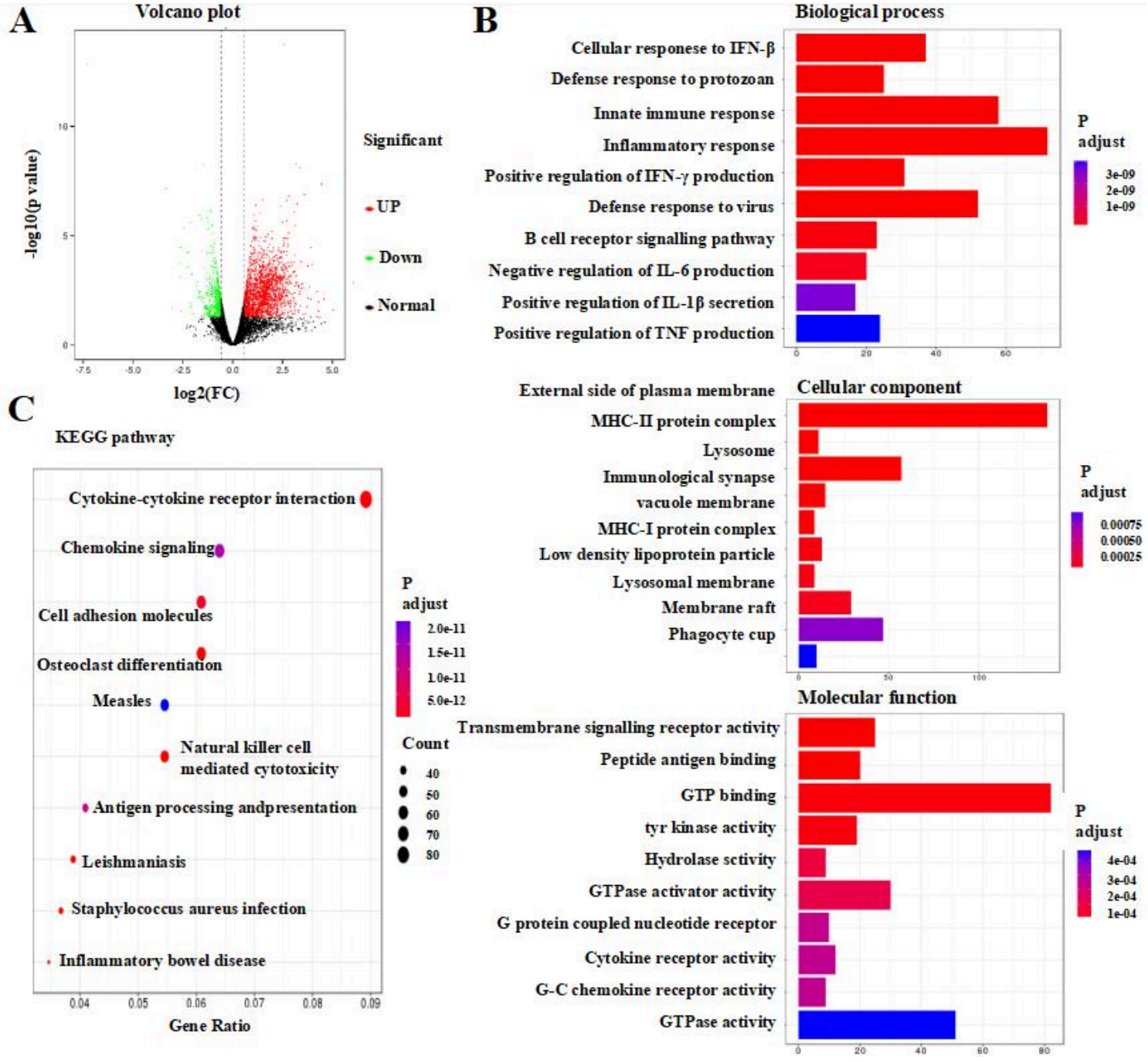


Figure 3

RNA-seq analysis of the expression profiles of differentially expressed genes in immune-related pathways. differential gene volcano plot, Compared with the Control group, a total of 2326 differential genes were detected, of which 1,810 were upadjusted genes and 516 were down-adjusted genes(A).

Histogram of Go enrichment of all differential genes (B). The most significant 30 Term scatter plots with GO enrichment in GUPS-DC+HPV vs Control groups (C).

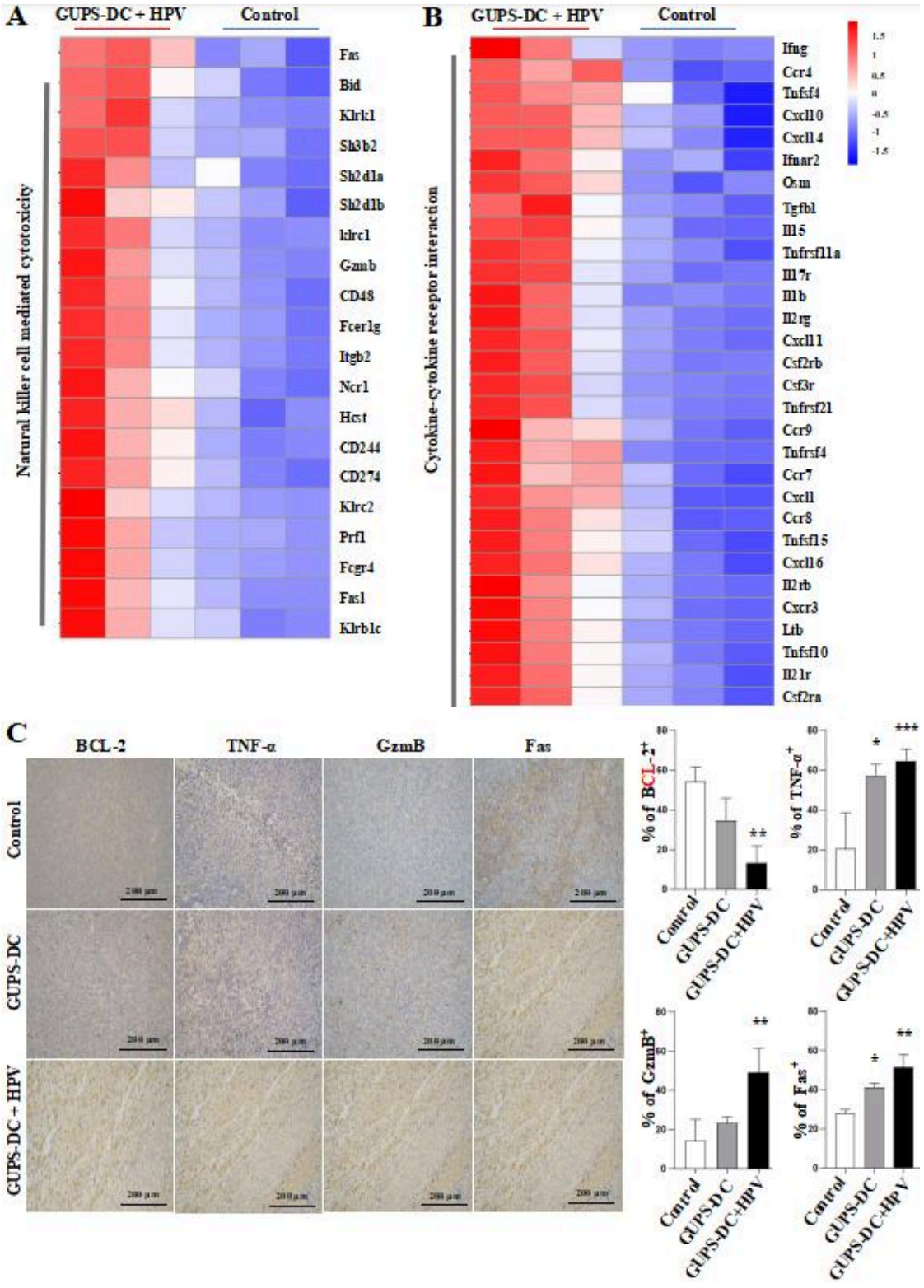


Figure 4

Perform RNA sequencing analysis on the expression profiles of differentially expressed genes in immune-related pathways. Cluster analysis of the expression profiles of differentially expressed genes in

the pathway related to natural killer cell-mediated cytotoxicity (A). Cluster analysis of the expression profiles of differentially expressed genes in the pathway related to cytokine-cytokine receptor interaction (B). Immunohistochemical staining images of *BCL-2, TNF-α, GzmB and Fas* in mouse tumor tissue array (magnification of 200) (4C).(*$P < 0.05$, **$P < 0.01$, ***$P < 0.001$ versus the control group).

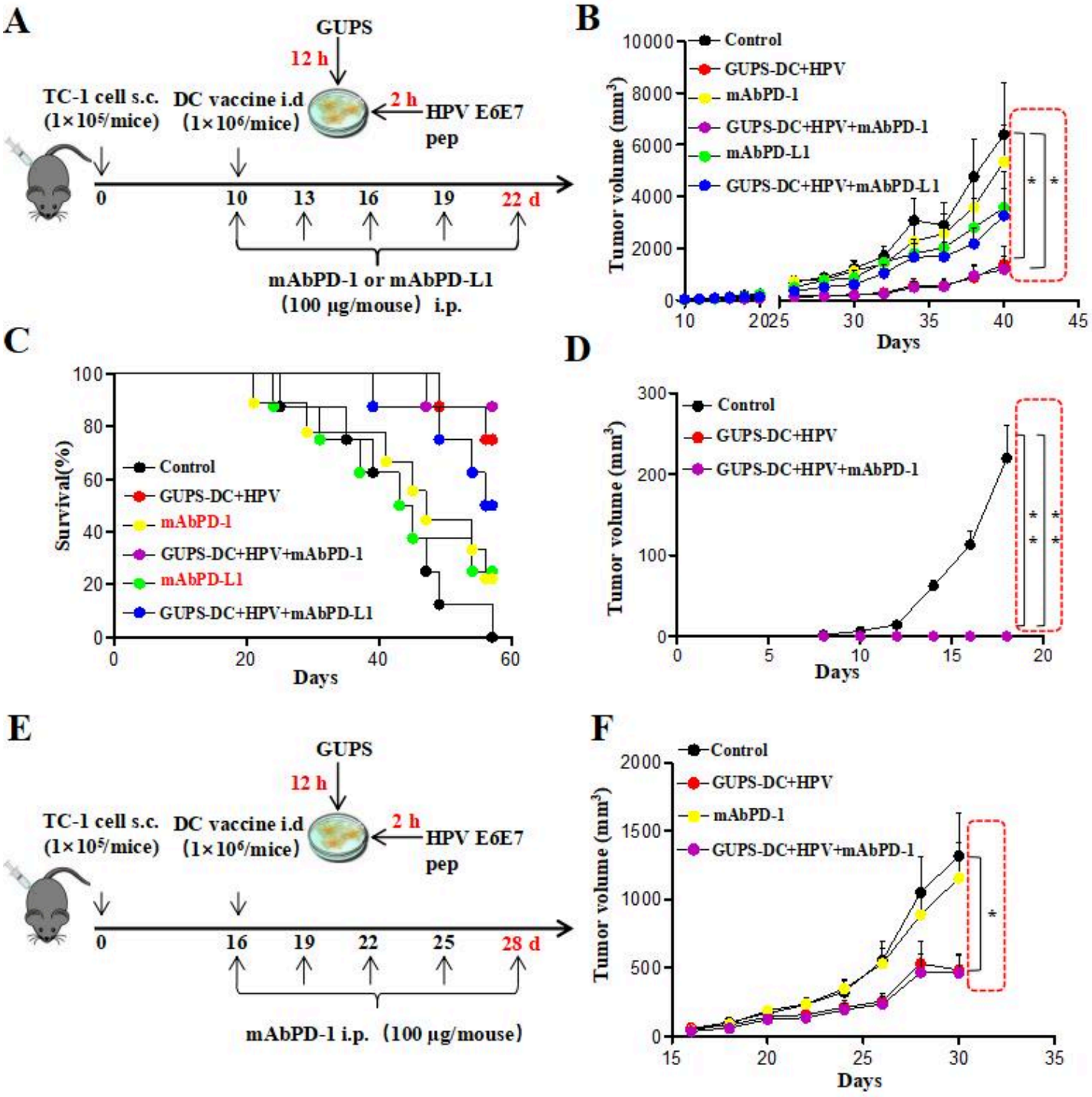


Figure 5

Treatment of tumor mice by GUPS-DC+HPV combined with mAbPD-1 or mAbPD-L1.The therapeutic strategy for mice (A) .Tumor mice were treated with GUPS-DC+HPV on day 10 and treated with mAbPD-1or mAbPD-L1 on days 10, 13, 16, 19, 22, then Tumor size and body weight was measured every other day,the survival of tumor mice was monitored.Tumor growth curves reflected by the average tumor volume during the period of immunization(B). The survival of tumor mice after GUPS-DC+HPV treatment (C). Tumor volumes were measured of the memory immune responses in mice (D). To evaluate the effect of GUPS-DC+ HPV combined with PD-1 antibody treatment in the advanced treatment of tumor mice. On the 10 th day after the establishment of TC-1 tumor model, On the 16th day, intradermal injection of GUPS-DC+HPV was used as the GUPS-DC+HPV group. mAbPD-1 (100 μg/ animal) were intraperitoneally injected into the mAbPD-1 group on the 16th, 19th, 22th, 25th and 28th days (E).Tumor growth curves reflected by the average tumor volume during the period of immunization (F). (*P < 0.05, **P < 0.01, ***P < 0.001 versus the control group).

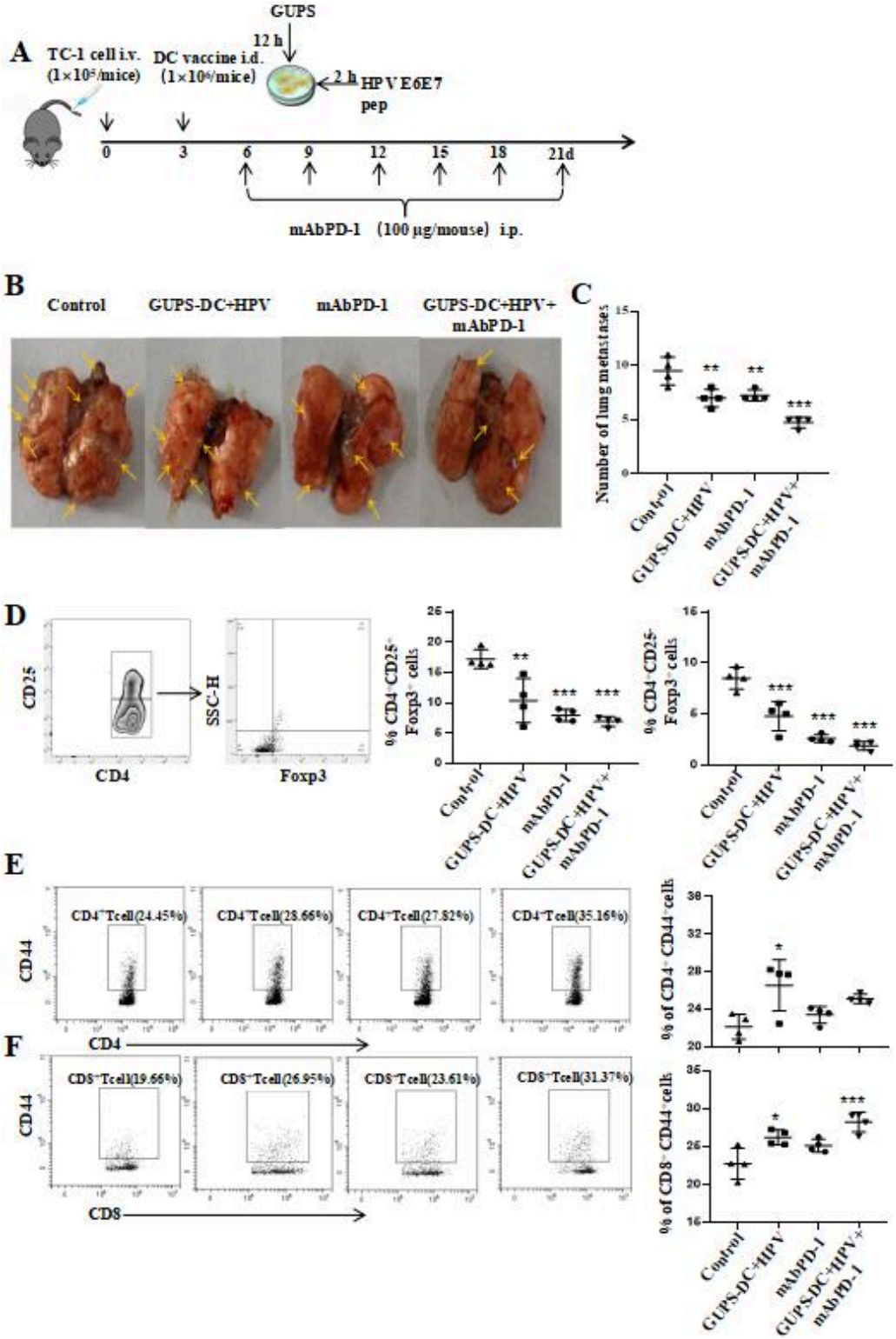


Figure 6

GUPS-DC+HPV combined with mAbPD-1 or mAbPD-L1 to treat lung metastatic tumor mice. Tumor mice were treated with GUPS-DC+HPV on day 3 and treated with mAbPD-1 or mAbPD-L1 on days 6, 9, 12, 15, 19, 21, then body weight was measured every other day(A). Pictures of cervical cancer, tail vein injection and metastasis to the lungs (B) .Statistics on the number of lung metastases (C). The immune responses in TC-1 tumor mice after treatment with GUPS-DC+HPV+mAbPD1, The frequencies of

immune cells in spleens. The effect of GUPS-DC+HPV+mAbPD1 on Treg cells $CD4^{+}CD25^{+}Foxp3^{+}$ cells (D). Proportion of activated $CD4^{+}$T cells($CD19b^{-}CD3^{+}CD4^{+}CD44^{+}$) and activated $CD8^{+}$T cells ($CD19b^{-}CD3^{+}CD8^{+}CD44^{+}$). (*$P$ < 0.05, **P < 0.01, ***P < 0.001 versus the control group).